

## Article

# Ab Initio Investigation of Helium Mobility in La<sub>2</sub>Zr<sub>2</sub>O<sub>7</sub> Pyrochlore

Yanxia Lu <sup>1</sup>, Qing Peng <sup>2</sup>  and Chenguang Liu <sup>1,\*</sup><sup>1</sup> School of Nuclear Equipment & Nuclear Engineering, Yantai University, Yantai 264005, China; luyanxia@ytu.edu.cn<sup>2</sup> Physics Department, King Fahd University of Petroleum & Minerals, Dhahran 31261, Saudi Arabia; Qing.Peng@kfupm.edu.sa

\* Correspondence: liuchg13@lzu.edu.cn

**Abstract:** The  $\alpha$ -decay of incorporated actinides continuously produces helium, resulting in helium accumulation and causing security concerns for nuclear waste forms. The helium mobility is a key issue affecting the accumulation and kinetics of helium. The energy barriers and migration pathways of helium in a potential high-level nuclear waste forms, La<sub>2</sub>Zr<sub>2</sub>O<sub>7</sub> pyrochlore, have been investigated in this work using the climbing image nudged elastic band method with density functional theory. The minimum energy pathway for helium to migrate in La<sub>2</sub>Zr<sub>2</sub>O<sub>7</sub> is identified as via La–La interstitial sites with a barrier of 0.46 eV. This work may offer a theoretical foundation for further prospective studies of nuclear waste forms.

**Keywords:** helium; mobility; La<sub>2</sub>Zr<sub>2</sub>O<sub>7</sub>; ab initio



**Citation:** Lu, Y.; Peng, Q.; Liu, C. *Ab Initio Investigation of Helium Mobility in La<sub>2</sub>Zr<sub>2</sub>O<sub>7</sub> Pyrochlore*. *Crystals* **2021**, *11*, 667. <https://doi.org/10.3390/cryst11060667>

Academic Editors: Indrajit Charit and Thomas M. Klapötke

Received: 22 May 2021

Accepted: 31 May 2021

Published: 10 June 2021

**Publisher's Note:** MDPI stays neutral with regard to jurisdictional claims in published maps and institutional affiliations.



**Copyright:** © 2021 by the authors. Licensee MDPI, Basel, Switzerland. This article is an open access article distributed under the terms and conditions of the Creative Commons Attribution (CC BY) license (<https://creativecommons.org/licenses/by/4.0/>).

## 1. Introduction

The safe disposition of the minor actinides and plutonium (Pu) generated from spent fuel, nuclear waste and dismantled nuclear weapons has become an important challenge in the development of nuclear industry [1,2]. Pyrochlores have attracted tremendous attention as a potential host matrix to immobilize minor actinides and Pu [3–5]. Most studies have paid more attention to evaluating the effects of radiation on these solids. However, the  $\alpha$ -decay of incorporated actinides also produces helium (He), which is ignored. As the accumulated He will cause swelling and mitigate the physical properties of pyrochlores [6–10], it is essential to study He solubility, diffusion, trapping and release in pyrochlores.

La<sub>2</sub>Zr<sub>2</sub>O<sub>7</sub> pyrochlore, as a candidate nuclear waste form, was selected to study the effects of He in pyrochlores and compare the differences of He behavior in different local environments based on our previous work [8]. The results show that the local environment has little influence on the behaviors of He, and the octahedral interstitial sites are the preferred positions for He to occupy in La<sub>2</sub>Zr<sub>2</sub>O<sub>7</sub> pyrochlore. Structural distortion and volume swelling have also been observed in He–La<sub>2</sub>Zr<sub>2</sub>O<sub>7</sub> systems. Similar research of He behavior in Y<sub>2</sub>Ti<sub>2</sub>O<sub>7</sub> pyrochlore was performed by Danielson et al. [10] using first principles calculation. They analyzed the effects of He interstitials on structural and electronic properties of Y<sub>2</sub>Ti<sub>2</sub>O<sub>7</sub> pyrochlore, and the results revealed that the oxygen orbital distortion induced by the presence of He resulted in the change in Ti–O bond character and structural deformation. In their other work [11], the mobility of He in Y<sub>2</sub>Ti<sub>2</sub>O<sub>7</sub> pyrochlore was also investigated using density functional theory. They calculated the migration barriers and plotted the potential energy landscape for He in pyrochlore and concluded that the deep potential energy wells lead He atoms to be trapped at the octahedral sites. In addition, the climbing image nudged elastic band (CI-NEB) method was adopted in their work and confirmed that the O–O interstitial was the transition state between two octahedral sites.

Recently, the combined effects of radiation and He accumulation have been simulated in experiments using ion irradiation and He implantation. For example, in Taylor et al.'s [6]

study,  $\text{Gd}_2\text{Zr}_2\text{O}_7$  pyrochlore was pre-damaged using 7 MeV  $\text{Au}^{3+}$  and then implanted into different concentrations of He, and the results showed the lattice swelling and He bubble chains in their samples. In their other similar work [7], individual He bubbles appeared after implantation with 12 at.% He in  $\text{Gd}_2\text{Ti}_2\text{O}_7$  pyrochlore, but without fracturing the solid. Additionally, Huang et al. [9] found that nanograin  $\text{Gd}_2\text{Zr}_2\text{O}_7$  ceramic can delay the process of He bubble evolution due to the presence of large grain boundary areas in the material.

The mobility and the migration barriers of He in the complex oxide  $\text{La}_2\text{Zr}_2\text{O}_7$  are still unclear. This work presents systemic research on the mobility of He in  $\text{La}_2\text{Zr}_2\text{O}_7$  pyrochlore to confirm the migration barriers and the transition state between different He interstitial locations, which will provide a theoretical reference for further understanding the relationship between He atoms and the coalescence of larger He bubbles. In addition, the mechanical stability of  $\text{La}_2\text{Zr}_2\text{O}_7$  containing different concentrations of He have been evaluated in this work. The method we used in this work, the results and discussion will be illustrated in Sections 2 and 3, respectively. In Section 4, we will summarize the current work.

## 2. Computational Method

All DFT calculations were performed with the Vienna Ab Initio Simulation Package (VASP) [12,13] with the projector augmented wave method (PAW) [14] pseudopotentials. Generalized gradient approximation (GGA) from Perdew–Burke–Ernzerhoff (PBE) [15] was selected to describe the exchange–correlation functional of the valence electrons. The  $4 \times 4 \times 4$   $k$ -point mesh for the He– $\text{La}_2\text{Zr}_2\text{O}_7$  systems containing 89 atoms with a Monkhorst–Pack scheme was adopted for the Brillouin zone sampling. The plane-wave cutoff energy was 478.9 eV, and the total energy and total force were converged to  $10^{-5}$  eV and 0.01 eV/Å in structural relaxation, respectively. The migration barriers of He in the two complex oxides were calculated using the climbing image nudged elastic band method [16,17].

## 3. Results and Discussion

### 3.1. Atomic Structures

The climbing image nudged elastic band method has been applied to calculate the migration barriers of He in pyrochlore [11]. The interstitial location with higher energy has always been regarded as a possible transition state, and the location with the lowest energy has always been assumed to be the final state. The octahedral interstitial site with the lowest formation energy (see Table 1) is the preferred position for He to occupy, and it is used for the final state in the He– $\text{La}_2\text{Zr}_2\text{O}_7$  system. To investigate the migration barriers and the migration paths of He, different cases were tested and calculated, i.e., the helium atom travels from the unstable interstitial positions with higher formation energy to another adjacent octahedral interstitial site. Here, the La–La (He atom at the midpoint of two lanthanum atoms), O–O (He atom at the midpoint of two oxygen atoms) and Tet. (He atom at the tetrahedral location) interstitial locations (see Figure 1) were considered, and each of them could be a possible energetic path for He atoms to diffuse in  $\text{La}_2\text{Zr}_2\text{O}_7$  pyrochlore. The site of a He atom at the midpoint of two Zr atoms (Zr–Zr) is also treated as the tetrahedral interstitial site, because the Zr–Zr interstitial relaxes into the tetrahedral position, and they maintain considerable formation energies [8].

**Table 1.** Formation energies of helium atom at interstitial sites.

Site		La–La	O–O	Zr–Zr	Tet.	Oct.
Formation Energy (eV)	He–La <sub>2</sub> Zr <sub>2</sub> O <sub>7</sub>	1.80	2.69	2.02	2.01	1.60

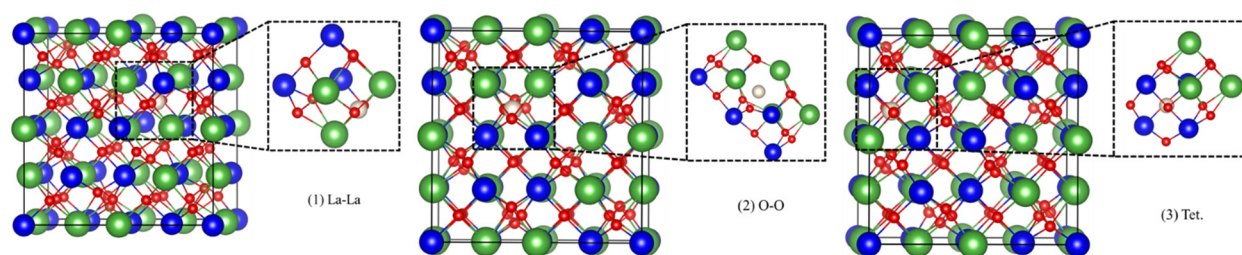


**Figure 1.** The structure of He- $\text{La}_2\text{Zr}_2\text{O}_7$  system for initial state. The green, blue, red and ivory spheres represent La, Zr, O and He atoms, respectively. (1) La-La (He atom at the midpoint of two lanthanum atoms), (2) O-O (He atom at the midpoint of two oxygen atoms), (3) Tet. (He atom at the tetrahedral location).

### 3.2. Migration Paths and Barriers of He in $\text{La}_2\text{Zr}_2\text{O}_7$

The first case we considered is when a He atom passes through the La-La interstitial to reach an adjacent octahedral interstitial site. The migration pathway of a He atom and the potential energy relative to the initial state is shown in Figure 2(1) with an energy barrier of 0.26 eV. The middle state with the highest energy exists between the La-La interstitial site and Oct. interstitial site, corresponding to the reaction coordinate 1.72 Å. Within the process of He atom diffusion, local spatial structure distortion has also been observed. In the second case, the migration energy barrier for a He atom to migrate from the Tet. site to an adjacent Oct. site is 0.39 eV, as shown in Figure 2(2). The configuration with the highest energy was observed at 0.93 Å along the reaction coordinate between the Tet. site and the Oct. site. Similarly, the He atom caused the change in the local structure, which was induced by the interaction between He and surrounding atoms and then resulted in the local changes of electronic structures and chemical bond in  $\text{La}_2\text{Zr}_2\text{O}_7$  pyrochlore [8].

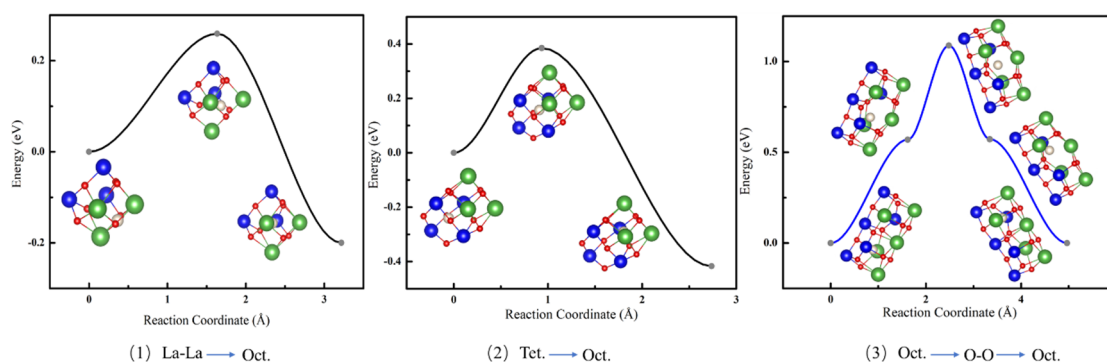


**Figure 2.** Migration pathway for He atom from (1) La-La interstitial site, (2) tetrahedral interstitial site and (3) O-O interstitial site to octahedral interstitial site. The local  $\text{La}_2\text{Zr}_2\text{O}_7$  pyrochlore structures including a He atom are illustrated in the figure, the green, blue, red and ivory spheres represent La, Zr, O and He atoms, respectively.

The last case is when a He atom migrates from the O-O site to an Oct. site, as shown in Figure 2(3). It shows that the O-O interstitial site is a unstable site and spontaneously degenerates to the octahedral interstitial site, with an energy difference of 1.09 eV, which is considered as the energy barrier for the path of Oct.-O-O-Oct. This trend can also be derived from Table 1, which shows that a He atom at the midpoint of two oxygen atoms has the highest formation energy in the He- $\text{La}_2\text{Zr}_2\text{O}_7$  system. By analyzing the energy difference between the initial state and final state, the most favorable path for He to diffuse from the octahedral site to a neighboring octahedral site in  $\text{La}_2\text{Zr}_2\text{O}_7$  pyrochlore is through the La-La interstitial site with an energy barrier of 0.46 eV.

#### 4. Mechanical Properties

To clarify the possible impact of a helium atom at different positions on the mechanical properties of  $\text{La}_2\text{Zr}_2\text{O}_7$  pyrochlore, the elastic constants and bulk moduli have been calculated for different helium interstitial configurations of He- $\text{La}_2\text{Zr}_2\text{O}_7$ . The elastic constants for cubic crystals,  $C_{11}$ ,  $C_{12}$  and  $C_{44}$ , are obtained from the first derivative of the fit to the stress-strain relationships (see ref. [11] for more details). Then, the bulk modulus ( $B$ ) and shear modulus ( $G$ ) can be estimated according to the Voigt-Reuss-Hill approximation [11] using the following equation:

$$B = (C_{11} + 2C_{12})/3$$

$$G = \left( \frac{C_{11} - C_{12} + 3C_{44}}{5} + \frac{5(C_{11} - C_{12})C_{44}}{4C_{44} + 3(C_{11} - C_{12})} \right) / 2$$

Furthermore, Young's modulus ( $E$ ) and Poisson's ratio ( $\nu$ ) can be calculated using the equations:

$$E = 9BG / (3B + G)$$

$$\nu = \frac{3B - 2G}{2(3B + G)}$$

The calculated results together with available experimental and theoretical values are shown in Table 2. All the elastic constants satisfy the following elastic stability criteria according to the Born rule:

$$C_{11} + 2C_{12} > 0$$

$$C_{44} > 0$$

$$C_{11} - C_{12} > 0$$

**Table 2.** Elastic constants ( $C_{11}$ ,  $C_{12}$ ,  $C_{44}$ ), bulk modulus ( $B$ ), shear modulus ( $G$ ) and Young's modulus ( $E$ ) for He- $\text{La}_2\text{Zr}_2\text{O}_7$ . Here, a He atom is at the La-La (He atom at the midpoint of two lanthanum atoms), O-O (He atom at the midpoint of two oxygen atoms), Tet. (He atom at the tetrahedral location) and Oct. (He atom at the octahedral location) interstitial locations. The unit for all values is GPa.

	$C_{11}$	$C_{12}$	$C_{44}$	$B$	$G$	$E$	$\nu$
$\text{La}_2\text{Zr}_2\text{O}_7$	261.72	103.58	84.10	156.29	82.05	209.49	0.277
Exp. [18]				171			
Cal. [19]	289	124	100	179		214	
La-La	275.27	101.22	89.32	159.24	88.39	223.78	0.266
O-O	253.04	103.09	68.68	153.07	71.13	184.78	0.299
Tet.	267.04	103.10	82.32	157.74	82.18	210.06	0.278
Oct.	262.63	105.16	84.05	157.65	81.88	209.39	0.279

This means that  $\text{La}_2\text{Zr}_2\text{O}_7$  pyrochlore and He- $\text{La}_2\text{Zr}_2\text{O}_7$  systems are mechanically stable, and a single helium interstitial will have no significant effect on the mechanical stability of  $\text{La}_2\text{Zr}_2\text{O}_7$  pyrochlore. From Table 2, there is a weak increase/(decrease) in  $B$ ,  $G$  and  $E$  caused by the presence of helium atom at the La-La site/(O-O site). This may be related to the interaction between a helium and oxygen atom and the dissymmetrical changes in  $\langle \text{La-O} \rangle$  bonds [8].

#### 5. Conclusions

The migration paths and energy barriers of He in  $\text{La}_2\text{Zr}_2\text{O}_7$  pyrochlore have been investigated systemically using the climbing image nudged elastic band method within a density functional theory framework. In the He- $\text{La}_2\text{Zr}_2\text{O}_7$  system, the most favorable path for He to diffuse is from an octahedral site to a neighboring octahedral site through the La-La interstitial site with an energy barrier of 0.46 eV. The diffusion of He in  $\text{La}_2\text{Zr}_2\text{O}_7$  pyrochlore can distort the local structure due to the interaction between the He atom and surrounding atoms. The understanding of He interstitial migration provides insight into

the behavior of He in pyrochlores. This will improve the theoretical research of pyrochlore in the field of high-level nuclear waste forms.

**Author Contributions:** Conceptualization, C.L. and Q.P.; methodology, C.L. and Q.P.; software, C.L.; validation, Y.L., C.L. and Q.P.; formal analysis, Y.L., C.L.; investigation, Y.L., C.L. and Q.P.; writing—original draft preparation, Y.L., C.L.; writing—review and editing, C.L. and Q.P.; visualization, C.L.; funding acquisition, C.L. and Q.P. All authors have read and agreed to the published version of the manuscript.

**Funding:** This research was funded by the National Natural Science Foundation of China, grant number 11875046, “the start-up fund from Yantai University to C.L., grant number HD20B02” and “the support provided by the Deanship of Scientific Research (DSR) at King Fahd University of Petroleum & Minerals (KFUPM), grant number DF201020.”

**Institutional Review Board Statement:** Not applicable.

**Informed Consent Statement:** Not applicable.

**Acknowledgments:** This work was supported by the National Natural Science Foundation of China (No.11875046) and the start-up fund from Yantai University to C.L. (No. HD20B02). Q.P. would like to acknowledge the support provided by the Deanship of Scientific Research (DSR) at King Fahd University of Petroleum & Minerals (KFUPM) through project No. DF201020.

**Conflicts of Interest:** The authors declare no conflict of interest.

## References

1. Ewing, R.C. Nuclear waste forms for actinides. *Proc. Natl. Acad. Sci. USA* **1999**, *96*, 3432–3439. [[CrossRef](#)] [[PubMed](#)]
2. Ewing, R.C.; Weber, W.J.; Lian, J. Nuclear waste disposal—Pyrochlore ( $A_2B_2O_7$ ): Nuclear waste form for the immobilization of plutonium and “minor” actinides. *J. Appl. Phys.* **2004**, *95*, 5949–5971. [[CrossRef](#)]
3. Weber, W.J.; Ewing, R.C. Plutonium Immobilization and Radiation Effects. *Science* **2000**, *289*, 2051–2052. [[CrossRef](#)] [[PubMed](#)]
4. Sickafus, K.E.; Minervini, L.; Grimes, R.W.; Valdez, J.A.; Ishimaru, M.; Li, F.; McClellan, K.J.; Hartmann, T. Radiation Tolerance of Complex Oxides. *Science* **2000**, *289*, 748–751. [[CrossRef](#)] [[PubMed](#)]
5. Weber, W.J.; Navrotsky, A.; Stefanovsky, S.; Vance, E.R.; Vernaz, E. Materials Science of High-Level Nuclear Waste Immobilization. *MRS Bull.* **2011**, *34*, 46–53. [[CrossRef](#)]
6. Taylor, C.A.; Patel, M.K.; Aguiar, J.A.; Zhang, Y.; Crespillo, M.L.; Wen, J.; Xue, H.; Wang, Y.; Weber, W.J. Bubble formation and lattice parameter changes resulting from He irradiation of defect-fluorite  $Gd_2Zr_2O_7$ . *Acta Mater.* **2016**, *115*, 115–122. [[CrossRef](#)]
7. Taylor, C.A.; Patel, M.K.; Aguiar, J.A.; Zhang, Y.; Crespillo, M.L.; Wen, J.; Xue, H.; Wang, Y.; Weber, W.J. Combined effects of radiation damage and He accumulation on bubble nucleation in  $Gd_2Ti_2O_7$ . *J. Nucl. Mater.* **2016**, *479*, 542–547. [[CrossRef](#)]
8. Liu, C.G.; Li, Y.H.; Li, Y.D.; Dong, L.Y.; Wen, J.; Yang, D.Y.; Wei, Q.L.; Yang, P. First principle calculation of helium in  $La_2Zr_2O_7$ : Effects on structural, electronic properties and radiation tolerance. *J. Nucl. Mater.* **2018**, *500*, 72–80. [[CrossRef](#)]
9. Huang, Z.; Zhou, M.; Cao, Z.; Tang, Z.; Zhang, Y.; Duan, J.; Qi, J.; Guo, X.; Lu, T.; Wu, D. He irradiation-induced lattice distortion and surface blistering of  $Gd_2Zr_2O_7$  defect-fluorite ceramics. *J. Am. Ceram. Soc.* **2020**, *103*, 3425–3435. [[CrossRef](#)]
10. Danielson, T.; Hin, C. Structural and electronic effects of helium interstitials in  $Y_2Ti_2O_7$ : A first-principles study. *J. Nucl. Mater.* **2014**, *452*, 189–196. [[CrossRef](#)]
11. Danielson, T.; Tea, E.; Hin, C. Ab initio investigation of helium in  $Y_2Ti_2O_7$ : Mobility and effects on mechanical properties. *J. Nucl. Mater.* **2016**, *477*, 215–221. [[CrossRef](#)]
12. Kresse, G.; Furthmüller, J. Efficiency of ab-initio total energy calculations for metals and semiconductors using a plane-wave basis set. *Comput. Mater. Sci.* **1996**, *6*, 15–50. [[CrossRef](#)]
13. Kresse, G.; Furthmüller, J. Efficient iterative schemes for ab initio total-energy calculations using a plane-wave basis set. *Phys. Rev. B* **1996**, *54*, 11169–11186. [[CrossRef](#)] [[PubMed](#)]
14. Blochl, P.E. Projector augmented-wave method. *Phys. Rev. B Condens. Matter* **1994**, *50*, 17953–17979. [[CrossRef](#)] [[PubMed](#)]
15. Perdew, J.P.; Burke, K.; Ernzerhof, M. Generalized Gradient Approximation Made Simple. *Phys. Rev. Lett.* **1996**, *77*, 3865–3868. [[CrossRef](#)] [[PubMed](#)]
16. Jónsson, H.; Mills, G.; Jacobsen, K.W. Nudged Elastic Band Method for Finding Minimum Energy Paths of Transitions; Classical and Quantum Dynamics in Condensed Phase Simulations. *June* **1998**, 385–404.
17. Henkelman, G.; Uberuaga, B.P.; Jónsson, H. A climbing image nudged elastic band method for finding saddle points and minimum energy paths. *J. Chem. Phys.* **2000**, *113*, 9901. [[CrossRef](#)]
18. Wan, C.L.; Pan, W.; Xu, Q.; Qin, Y.X.; Wang, J.D.; Qu, Z.X.; Fang, M.H. Effect of point defects on the thermal transport properties of  $(La_xGd_{1-x})_2Zr_2O_7$ : Experiment and theoretical model. *Phys. Rev. B* **2006**, *74*, 144109. [[CrossRef](#)]
19. Liu, B.; Wang, J.Y.; Zhou, Y.C.; Liao, T.; Li, F.Z. Theoretical elastic stiffness, structure stability and thermal conductivity of  $La_2Zr_2O_7$  pyrochlore. *Acta Mater.* **2007**, *55*, 2949–2957. [[CrossRef](#)]